The Geometry of Sagittarius Stream from Pan-STARRS1 3π RR Lyrae

Nina Hernitschek[1,2], Branimir Sesar[2], Hans-Walter Rix[2] and Judith G. Cohen[1]

1. Division of Physics, Mathematics and Astronomy, Caltech, Pasadena, CA 91125d
2. Max-Planck-Institut für Astronomie, Königstuhl 17, 69117 Heidelberg, Germany

We present an analysis of the Sagittarius (Sgr) stellar stream's 3D geometry, based on the sample of ∼44 000 RR Lyrae (RRab) stars from the Pan-STARRS1 (PS1) 3π survey, extending to $\gtrsim$120 kpc with a distance precision of ∼3%. A projection of RR Lyrae stars within $|\tilde{B}|_\odot < 9^\circ$ of the Sgr stream's orbital plane reveals the morphology of both the leading and the trailing arms at very high contrast. We fit a model for the angular mean distance and line-of-sight depth, resulting in estimates of the mean stream distance precise to ∼1% and resolving the stream's line-of-sight depth. These improved geometric constraints can serve as new restrictions for dynamical stream models.

1 Introduction

Stellar streams are of great interest as their orbits are sensitive tracers of the Milky Way's formation history and gravitational potential (e.g. Law & Majewski, 2010; Sanders & Binney, 2013). The Sagittarius (Sgr) stream is the dominant tidal stellar stream of the Galactic stellar halo, showing two pronounced tidal tails, each trail extending ∼180° and reaching Galactocentric distances from 20 to more than 100 kpc. Since its discovery by Ibata et al. (1994), there have been many attempts to map and trace the Sgr stream. In more recent work, Belokurov et al. (2014) have traced its trailing arm out to its apocenter at ∼100 kpc. The extent of the Sgr stream has, therefore, only recently became fully apparent, spanning an unparalleled range of distances compared to other stellar tidal streams. There are also attempts to model the stream using N-body simulations constrained by observational data (e.g. Law & Majewski, 2010; Dierickx & Loeb, 2017).

The aim of this work is to map the geometry of the Sgr stream more precisely, accurately, and comprehensively than before, using exclusively RRab stars from a single survey while tracing the complete angular extent of the Sgr stream as well as to look even to the outskirts of the stream.

2 Data

For our analysis, we use the RRab sample of Sesar et al. (2017), which covers 3/4 of the sky, contains 44 403 sources, is pure at ∼80% out to 80 kpc, and has precise distances (to 3%). It was generated from the PS1 survey (Chambers et al., 2016), using structure functions and a machine-learning algorithm (Hernitschek et al., 2016) as well as multi-band light-curve fitting and machine-learning algorithms (Sesar et al.,

2017). Using heliocentric Sagittarius coordinates $(\tilde{\Lambda}_\odot, \tilde{B}_\odot)$ as defined by Belokurov et al. (2014), we restrict or sample to sources within 9° of the equator, $|\tilde{B}_\odot| < 9°$, resulting in ∼15 000 stars as shown in Fig. 1.

3 A Simple Model to Characterize the Sgr Stream Geometry

We model the overall distance distribution $p_{\rm RRL}(D)$ towards any $\tilde{\Lambda}_\odot$ as the superposition of a Gaussian ($D_{\rm sgr}$, $\sigma_{\rm sgr}$) "stream" and power-law "halo" component:

$$p_{\rm RRL}(\mathcal{D}|\boldsymbol{\theta}) = p_{\rm halo}(\mathcal{D}|\boldsymbol{\theta}) + p_{\rm stream}(\mathcal{D}|\boldsymbol{\theta}) \quad (1)$$

$$= (1 - f_{\rm sgr}) \times \hat{\rho}_{\rm halo}(l, b, D, q, n) + f_{\rm sgr} \times \hat{\rho}_{\rm sgr}(l, b, D, D_{\rm sgr}, \sigma_{\rm sgr}) \quad (2)$$

where $\hat{\rho}_{\rm halo}(l, b, D, q, n)$, $\hat{\rho}_{\rm stream}(l, b, D, q, n)$ are the normalized halo and stream densities. The data set is given as $\mathcal{D} = (D, \delta D, l, b)$. The parameters are $\boldsymbol{\theta} = (f_{\rm sgr}, D_{\rm sgr}, \sigma_{\rm sgr}, n)$, with $f_{\rm sgr}$ being the fraction of the stars associated with the Sgr stream at the given $\tilde{\Lambda}_\odot$ slice, the heliocentric distance of the stream $D_{\rm sgr}$, its line of sight depth $\sigma_{\rm sgr}$, and the power-law index n of the halo model.

The background of field stars is described by a power-law halo model $\rho_{\rm halo}$,

$$\rho_{\rm halo}(X, Y, Z) = \rho_{\odot \rm RRL} \left(R_\odot / r_q\right)^n \quad (3)$$

with

$$X = R_\odot - D \cos l \cos b,\ Y = -D \sin l \cos b,\ Z = D \sin b,\ r_q = \sqrt{X^2 + Y^2 + (Z/q)^2}.$$

The Galactocentric distance of the Sun is $R_\odot = 8.0\,{\rm kpc}$, the halo flattening along the Z direction is $q = 0.71$, and $\rho_{\odot \rm RRL} = 4.5\,{\rm kpc}^{-3}$ is the number density of RR Lyrae at the position of the Sun. The power-law index n is a fitting parameter.

The stream is modeled as a Gaussian centered on $D_{\rm sgr}$ and with variance $\sigma_{\rm sgr}$:

$$\rho_{\rm sgr}(l, b, D, \delta D, D_{\rm sgr}, \sigma_{\rm sgr}) = \frac{1}{\sqrt{2\pi(\sigma_{\rm sgr}^2 + \delta D^2)}} \exp\left(-\frac{(R(D) - R(D_{\rm sgr}))^2}{2(\sigma_{\rm sgr}^2 + \delta D^2)}\right) D^2.$$

For the distance uncertainties of RRab stars, we adopt $\delta D = 3\%$ (Sesar et al., 2017).

3.1 Fitting the Sgr Model

We split the sample of RRab stars into bins of $\tilde{\Lambda}_\odot \pm \Delta\tilde{\Lambda}_\odot/2$, each $\Delta\tilde{\Lambda}_\odot = 10°$ wide. In each, we fit the parameters of the stream and halo model n to the distances D. To constrain the geometry of the Sgr stream in a probabilistic manner, we calculate the joint posterior probability $p_{\rm RRL}(\boldsymbol{\theta}|\mathcal{D})$ of the parameter set $\boldsymbol{\theta} = (f_{\rm sgr}, D_{\rm sgr}, \sigma_{\rm sgr}, n)$, given the data set $\mathcal{D} = (D, \delta D, l, b)$. The marginal posterior probability $p_{\rm RRL}(\boldsymbol{\theta}|\mathcal{D})$ is related to the marginal likelihood $p_{\rm RRL}(\mathcal{D}|\boldsymbol{\theta})$ through $p_{\rm RRL}(\boldsymbol{\theta}|\mathcal{D}) \propto p_{\rm RRL}(\mathcal{D}|\boldsymbol{\theta}) p(\boldsymbol{\theta})$ where $p(\boldsymbol{\theta})$ is the prior probability of the parameter set. We evaluate $\ln p_{\rm RRL}(\boldsymbol{\theta}|\mathcal{D}) = \sum_i \ln p_{\rm RRL}(\mathcal{D}_i|\boldsymbol{\theta}) + \ln p(\boldsymbol{\theta})$ with $p_{\rm RRL}(\mathcal{D}_i|\boldsymbol{\theta})$ given by Eq. (2), and i indexes the RRab stars. Each distance and depth estimate $(D_{\rm sgr}, \sigma_{\rm sgr})$ is obtained by optimizing the posterior using a MCMC (Foreman-Mackey et al., 2013).

4 Results

In Fig. 1, the resulting geometric characterization of the Sgr stream is shown. It is apparent that the distance and line of sight depth estimate trace the stream well all the way out to more than 100 kpc. From this detailed picture of the Sgr stream, many features are obvious. The stream shows clearly distinct leading and trailing arms. The shape and extent look similar to what was found earlier (Belokurov et al., 2014). The leading arm's apocenter lies between $\tilde{\Lambda}_\odot = 60°$ and 70° where $D_{\rm sgr}$ reaches 49 kpc, and the trailing arm's apocenter is near $\tilde{\Lambda}_\odot{\sim}170°$ reaching its largest extent of 92 kpc. This agrees with Belokurov et al. (2014), who give the leading arm's apocenter being located at $\tilde{\Lambda}_\odot = (71.3 \pm 3.3)°$ and the trailing arm's apocenter at $\tilde{\Lambda}_\odot = (170.5 \pm 1)°$. At both the apocenters of the main leading arm ($\tilde{\Lambda}_\odot{\sim}70°$) and trailing arm ($\tilde{\Lambda}_\odot{\sim}180°$), our RRab map reveals substructure: two "clumps" (at $D{\sim}60$ and 80 kpc) beyond the leading arm's apocenter, and a "spur" of the trailing arm reaching up to 130 kpc, as predicted by (Dierickx & Loeb, 2017). These new Sgr stream features are discussed in Sesar et al. (2017) in detail.

4.1 The Line-of-Sight Depth of the Sagittarius Stream

The stream tends to broaden along its orbit from ∼1.75 kpc to 6 kpc for the leading arm, reaching even ∼10 kpc for the trailing arm. The leading arm's line of sight depth rises (and falls) towards (and away) from the apocenter. In contrast, $\sigma_{\rm sgr}$ for the trailing arm remains larger between $200° < \tilde{\Lambda}_\odot < 300°$. In part, this is presumably because our line-of-sight direction forms a shallower angle with the stream direction, compared to the leading arm. Except towards the apocenters, $\sigma_{\rm sgr}$ raises also towards the "end" (the largest $\tilde{\Lambda}_\odot$) of the respective trailing or leading arm.

As the angle between the normal on the stream and the line of sight is known, we deproject the line of sight depth $\sigma_{\rm sgr}$ to get the actual width of the stream, $\tilde{\sigma}_{\rm sgr}$. The $\tilde{\sigma}_{\rm sgr}$ profile is flatter than the $\sigma_{\rm sgr}$ profile, and as expected, the trailing arm's deprojected depth $\tilde{\sigma}_{\rm sgr}$ is not noticeably boosted in contrast to $\sigma_{\rm sgr}$ which is. A variation during the orbital period is still present. Comparing both depths emphasizes that the larger depth at the apocenters is a combination of the projection effect, as well as of the true broadening when the velocities become small near the apocenters.

4.2 The Apocenters and Orbital Precession of the Sagittarius Stream

Sources orbiting in a potential show a precession of their orbit, as the major axis of each orbit is rotating gradually within the orbital plane. Assuming a spherically symmetric potential, the precession depends primarily on the shape of the potential, and thus, the radial mass distribution (Belokurov et al., 2014).

The angular mean distance estimates $D_{\rm sgr}$ obtained during this work enable us to make statements about the precession of the orbit. We find the leading apocenter at $\tilde{\Lambda}^L_\odot = 63°$, $D^L_{\rm sgr} = 51$ kpc, and the trailing apocenter at $\tilde{\Lambda}^T_\odot = 167°$, $D^T_{\rm sgr} = 91$ kpc. The differential orbit precession $\omega_\odot = \tilde{\Lambda}^T_\odot - \tilde{\Lambda}^L_\odot$ is 104°, corresponding to a difference in heliocentric apocenter distances of 40 kpc. The opening angle between the positions of the two apocenters, as viewed from Galactic center, is $\omega_{\rm GC} = 97°$, and the difference in mean Galactocentric apocenter distances is 47 kpc.

4.3 The Orbital Plane Precession of the Sagittarius Stream

Aside from the apocenter precession of the stream, the orbital plane itself might show a precession. To test this, we obtain the weighted latitude of the stream RRab as a function of $\tilde{\Lambda}_\odot$. The weight of each star is the probability that the star is associated with the Sgr stream. The weighted latitude $\langle \tilde{B}_\odot \rangle$ in a bin i is then

$$\langle \tilde{B}_\odot \rangle_i = \frac{\sum_j (\tilde{B}_{\odot,i} \times p_{\mathrm{sgr},j})}{\sum_j (p_{\mathrm{sgr},j})},\ p_{\mathrm{sgr},j}(l_j, b_j, D_j|\boldsymbol{\theta}_i) = \frac{p_{\mathrm{stream}}(D|\boldsymbol{\theta}_i)}{p_{\mathrm{halo}}(D|\boldsymbol{\theta}_i) + p_{\mathrm{stream}}(D|\boldsymbol{\theta}_i)} \quad (4)$$

We use the difference in $\langle \tilde{B}_\odot \rangle$ for the leading and trailing arm to quantify the orbital plane precession, and find evidence for the leading arm staying in or close to the plane defined by $\tilde{B}_\odot = 0°$, whereas the trailing arm is found within within $-5°$ to $5°$ around the plane. This separation of $\sim$10° was also derived by Law et al. (2005).

5 Discussion and Summary

We can now put our results in the context of existing work, and discuss the prospect of using them for dynamical stream modeling. The best previous estimates of the heliocentric distances for a large part of the Sgr stream come from Belokurov et al. (2014), who used blue horizontal branch (BHB) stars, sub-giant branch (SGB) star, and red giant branch (RGB) stars from the SDSS DR8. Overall, the estimates from Belokurov et al. (2014) are in good agreement with our analysis. Their distances may be systematically slightly larger; the fact that the RRab distances we use are directly tied to *HST* and *Gaia* DR1 parallaxes (Sesar et al., 2017) should lend confidence to the distance scale of this work. To summarize the comparison:

- Our analysis is done from one single survey and type of stars, whereas the work by Belokurov et al. (2014) relies on BHB, SGB and RGB stars. Our work resulted in the first complete (i.e., spanning $0° < \tilde{\Lambda}_\odot < 360°$) trace of Sgr stream's heliocentric distance from a single type of stars originating from a single survey.
- The heliocentric mean distances of the stream as from Belokurov et al. (2014) may be systematically slightly larger; the fact that the RRab distances we use are directly tied to *HST* and *Gaia* DR1 parallaxes (Sesar et al., 2017) should lend confidence to the distance scale of this work.
- Along with the extent of the Sgr stream, we can give its line of sight depth σ_{sgr}, and deproject σ_{sgr} in order to get its true width.
- Our analysis shows a Galactocentric orbital precession being about 4° larger than as measured by Belokurov et al. (2014), or 8° larger if assuming the trailing arm's apocenter is close to the maximum extent of the derived D_{sgr}. This is within the error range given by Belokurov et al. (2014). This result, together with the result of Belokurov et al. (2014), as well as the simulation by Dierickx & Loeb (2017), is a strong indicator that a steeper profile than the logarithmic one should be considered for the dark matter halo of the Milky Way.

Having now a model of the geometry of the Sgr stream at hand, it can be used to further constrain the Milky Way's potential.

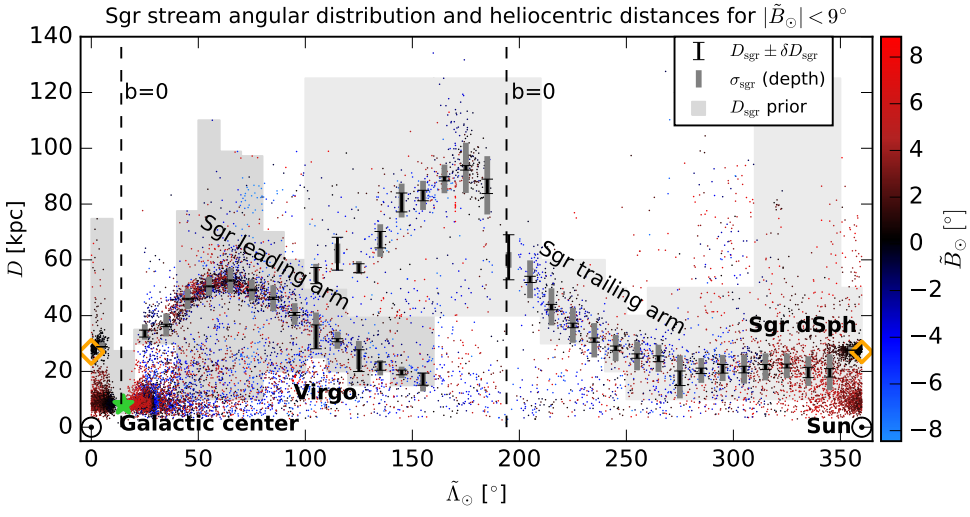

Fig. 1: The source distance distribution, overplotted with the fitted extent of the Sgr stream. The angular distance of the sources to the Sgr plane $\tilde{B}_\odot = 0°$ is indicated by color-coding; black points indicate the center of the $\tilde{\Lambda}_\odot$ slices used to estimate the distance $D_{\rm sgr}$. Dashed line marks the position of the Galactic plane.

References

Belokurov, V., Koposov, S. E., Evans, N. W., *MNRAS* **437**, 1 (2014)

Chambers, K. C., Magnier, E. A., Metcalfe, N., et al., *arXiv:1612.05560 [astro-ph.IM]* (2016)

Dierickx, M. I. P., Loeb, A., *ApJ* **836**, 92 (2017)

Foreman-Mackey, D., Hogg, D. W., Lang, D., Goodman, J., *PASP* **125**, 306 (2013), `arXiv:1202.3665`

Hernitschek, N., Rix, H.-W., Schlafly, E. F., et al., *ApJ* **817**, 73 (2016)

Ibata, R. A., Gilmore, G., Irwin, M. J., et al., *Nature* **370**, 194 (1994)

Law, D. R., Johnston, K. V., Majewski, S. R., *ApJ* **619**, 800 (2005)

Law, D. R., Majewski, S. R., *ApJ* **714**, 229 (2010)

Sanders, J. L., Binney, J., *MNRAS* **433**, 1826 (2013)

Sesar, B., Hernitschek, N., Mitrović, S., et al., *AJ* **153**, 204 (2017)